Transverse susceptibility as a probe of the magnetocrystalline anisotropy driven phase transition in $Pr_{0.5}Sr_{0.5}CoO_3$

N. A. Frey Huls[1, 2], N. S. Bingham[1], M. H. Phan[1], H. Srikanth[1], D. D. Stauffer[3], and C. Leighton[3]

[1]Department of Physics, University of South Florida, Tampa, Florida 33620, USA

[2]National Institute of Standards and Technology, Gaithersburg, Maryland 20899, USA

[3]Department of Chemical Engineering and Materials Science, University of Minnesota, Minneapolis, MN 55455, USA

Half-doped $Pr_{1-x}Sr_xCoO_3$ (x=0.5) displays anomalous magnetism most notably manifest in the field-cooled magnetization versus temperature curves under different applied cooling fields. Recently, an explanation was put forth that a magnetocrystalline anisotropy transition driven by a structural transition at 120K is the cause this behavior. In this paper, we further elucidate the nature of the magnetic anisotropy across this low temperature phase transition in this material by means of transverse susceptibility (TS) measurements performed using a self-resonant tunnel diode oscillator. TS scans as a function of field clearly reveal peaks associated with the anisotropy and switching fields. When peak placement is examined as a function of temperature around 120K, the signature of an FM-FM phase transition is evident as a sharp feature in H_K and a corresponding cusp in H_S. A new TS peak (not yet observed in other classes of magnetic oxides such as manganites and spinel ferrites) is correlated with the crossover field of the unusual M(T) behavior, and we demonstrate how TS peak magnitude can indicate easy axis switching in polycrystalline samples. Our results further confirm that TS can provide new insights into the magnetic behavior of complex oxides.

PACS: 75.30.Vn, 71.30.+h, 78.70.Ck, 72.40.+w

Key words: Cobaltites, Magnetocrystalline anisotropy, Magnetic switching

I. INTRODUCTION

Complex oxides of the general form $Ln_{1-x}AE_xTMO_3$ (Ln= Lanthanide, AE = Alkaline-Earth, TM = Transition Metal) have drawn intense interest from the magnetic community in recent years due to their unique properties such as charge ordering [1-3], structural transitions including Jahn-Teller distortion [4, 5], unusual magnetic and spin-flip transitions [6, 7], multiferroicity [8, 9], and magnetoelectronic phase separation [10, 11]. This makes them relevant in almost every area of magnetism including magnetoresistive sensors [12], spintronics due to their high spin polarization [13, 14], and magnetic refrigeration because of the large magnetocaloric effects they display [15, 16].

Until recently, the discussion associated with these perovskites has been largely dominated by the manganites (TM = Mn) because they have been known to exhibit all of these properties due to the interplay between charge, spin, lattice, and orbital degrees of freedom present leading to multiple ground states and transitions [17, 18]. But the relatively less-studied cobaltites (TM = Co) present interesting characteristics as well, perhaps the most well-known being the spin-state transition in $LaCoO_3$ [19-21]. Co substituted into the TM site leads to an additional spin-state degree of freedom due to similar crystal field and Hund's rule exchange energies. This along with a significantly larger magnetocrystalline anisotropy makes studying cobaltites intriguing both for fundamental physics and device applications in which manipulation of the anisotropy is desirable.

Half-doped $Pr_{1-x}Sr_xCoO_3$ (x=0.5) is known to exhibit particularly unusual magnetic behavior that is not consistent with phase transitions often seen in manganites and other complex oxide systems [22-26]. The field-cooled magnetization versus temperature profiles are the best example; at low cooling fields the magnetization first increases with decreasing temperature and then abruptly decreases with further decrease in temperature at around 120K (henceforth T_A). However with larger applied cooling fields, the magnetization first increases with decreasing temperature and then increases even more sharply at temperatures lower than T_A. The field-dependent M(T) behavior crosses over from decreasing below T_A to increasing below T_A at a field of around 75 mT, which we will refer to as H_{cr}. At cooling fields in which the magnetization is saturated, no anomaly is observed in the M(T). Figure 1 illustrates this phenomenon by showing field-cooled magnetization versus temperature for low cooling field (1 mT, 1a) intermediate cooling field (0.1 T, 1b) and saturated cooling field (5 T, 1c). Note that the decrease (increase) in magnetization upon cooling in low (high) field is manifest as a gradual change in curvature starting at around T_A and persists well into the low temperature regime.

In order to understand this paradoxical behavior, systematic studies were recently undertaken to rule out the phase transitions most routinely associated with perovskites such as charge ordering, antiferromagnetic ordering, or spin-flip transitions [27]. It was conclusively shown that all the observed behavior can be explained by a ferromagnetic to ferromagnetic (FM-FM) transition resulting from a small structural change which drives a transition in the magnetocrystalline anisotropy. Interestingly, this structural transition does not cause a change in crystal symmetry (both above and below T_A $Pr_{0.5}Sr_{0.5}CoO_3$ is monoclinic with space group $I2/a$) and the overall volume of the unit cell remains largely unaltered. However the a and b lattice

parameters undergo significant changes of +1.15% and -1.10% respectively upon cooling through the 120K transition, which alters the spin-orbital coupling via Pr-O hybridization and thus appears as a transition in the magnetocrystalline anisotropy. The result is two ferromagnetic phases consisting of a lower anisotropy phase (labeled FM1) at low temperature and a higher anisotropy phase (labeled FM2) at intermediate temperatures between T_A and T_C (T_C ~230K for $Pr_{0.5}Sr_{0.5}CoO_3$). Each of the two phases has distinct anisotropy features, which is the focus of the results presented in this paper.

Because this FM-FM transition is not clearly seen in transport measurements and traditional magnetometry measurements shed limited light on the nature of the magnetocrystalline anisotropy, we assert that the transverse susceptibility (TS) measurement technique – a reliable direct probe of the anisotropy and switching fields of a material – is extremely well-suited to explore this particular structure-driven magnetocrystalline anisotropy transition. We will also show that even H_{cr} is manifest in the transverse susceptibility profile and more readily quantifiable using this method.

Besides the drastic change in *magnitude* of the anisotropy of $Pr_{0.5}Sr_{0.5}CoO_3$ across T_A directly probed by TS experiments, we show that the changing magnitude of the directional- and field-dependent susceptibilities (H_{AC} perpendicular to H_{DC} and H_{AC} parallel to H_{DC}) also reveal the change in *direction* of the anisotropy. This is fully consistent with Lorentz microscopy [24] and traditional magnetometry [25] studies on single crystals of $Pr_{0.5}Sr_{0.5}CoO_3$ showing that there is a change in direction of the anisotropy vector with the easy axis of magnetization rotating from [110] at higher temperatures to [100] at low temperature.

II. EXPERIMENTAL DETAILS

Bulk, polycrystalline samples of $Pr_{0.5}Sr_{0.5}CoO_3$ were made according to the procedure outlined in reference [27]. In short, stoichiometric quantities of Pr_2O_3, $SrCO_3$, and Co_3O_4 were reacted at 1000°C for 7 days with several intermediate grindings followed by cold pressing, sintering at 1200°C for 1 day, and slow cooling (1°C/min) to room temperature. Extensive structural analysis, transport measurements and magnetic properties measurements were also carried out and discussed in reference [27].

Transverse susceptibility measurements were performed using a self-resonant tunnel diode oscillator with a resonant frequency of 12 MHz and sensitivity on the order of 10 Hz [28]. The tunnel diode oscillator is housed outside of a commercial Physical Properties Measurement System (PPMS, Quantum Design [29]) which serves to modulate the applied DC magnetic field ($\mu_0 H$ up to ±7 T) as well as the measurement temperature ($2K < T < 300K$). The sample goes into the inductance coil of the tank circuit which is integrated into the PPMS such that the perturbing RF magnetic field inside the coil ($\mu_0 H_{AC} \sim 1$ mT) is oriented perpendicular to the superconducting magnet. The transverse susceptibility (TS) measurement for a given temperature is performed by monitoring the change in the resonant frequency of the circuit as the DC field is swept from positive saturation to negative saturation and then back to positive (bipolar scan). Because the change in frequency of the circuit is a direct consequence of the change in inductance as the sample inside is magnetized, the quantity Δf is directly proportional to $\Delta \chi_T$. We are therefore most interested in the quantity

$$\frac{\Delta\chi_T}{\chi_T}(\%) = \frac{|\chi_T(H) - \chi_T^{sat}|}{\chi_T^{sat}} \times 100$$

as a function of H_{DC} where χ_T^{sat} is the transverse susceptibility at the saturating field H_{sat}. In accordance with Aharoni *et al.*'s theoretical predictions [30] we then see maxima in the TS scan at the positive and negative anisotropy fields of the material, $\pm H_K$, and one at the switching field, H_S for a unipolar sweep of the DC field from positive to negative saturation. This technique has been used with great success to examine the anisotropic magnetic properties of a variety of systems from multilayered thin films [31] to single crystals [32] and nanoparticles [33, 34]. However it also lends itself particularly well to the rich physics involved in complex oxide systems to examine the unusual magnetic behavior often seen in manganites [28, 32, 35, 36] and, as we show here, cobaltites.

III. RESULTS AND DISCUSSION

TS measurements were performed on a polycrystalline $Pr_{0.5}Sr_{0.5}CoO_3$ sample at a number of temperatures to examine the temperature dependence of the anisotropic features across the 120K transition. Figure 2 shows bipolar TS scans of $Pr_{0.5}Sr_{0.5}CoO_3$ taken at four representative temperatures: 20K (2a), 95K (2b), 110K (2c), and 225K (2d). Arrows have been inserted into figure 2c to indicate the sequence of measurement and the peaks discussed below have been labeled in figure 2a. The broader, high-field peaks seen on either side of $\mu_0 H=0$ closest to saturation are the anisotropy peaks indicating the anisotropy field, $\pm H_K$. The broad nature of the anisotropy peak can also ascribed to distribution in the anisotropy axis in polycrystalline

samples. Frequently, in physical systems that deviate from the theoretical conditions outlined in TS models and predictions, the H_K peaks are not located symmetrically about $\mu_0 H = 0$, differing both in magnitude and applied field value (i.e. $+H_K \neq -H_K$). In all such cases $-H_K$ is smaller in magnitude but occurs at higher field and is often broader in comparison to the $+H_K$ peak. This phenomenon is the subject of a previous study [34] and it is largely accepted that the differences in shape and placement of the $-H_K$ peak relative to the $+H_K$ peak in particulate systems is heavily dependent on such factors as inter-particle interactions, both dipolar and exchange in nature, as well as anisotropy and switching field distributions. A brief explanation for this is that the first anisotropy peak observed occurring after saturation arises under a different free-energy landscape than the second peak, which occurs after decreasing $\mu_0 H$ past the switching and coercive fields but before saturation in the opposite direction. For this reason, we consistently use $+H_K$ when referring to the anisotropy field. In the case of $Pr_{0.5}Sr_{0.5}CoO_3$, the $-H_K$ peak changes in shape over the temperature range studied; at low temperatures it is so smeared out as to be nearly impossible to determine its value. While we cannot make a direct comparison to the case of the particulate systems studied in reference [34], we note that analogous to interacting nanoparticle systems, polycrystalline samples experience inter-granular exchange interactions and different magnetic environments upon reaching saturation and subsequently passing through the coercive field, thus affecting the shape and magnitude of the $-H_K$ peak. In fact it has been observed [27] that the small low temperature magnetic susceptibility seen in the magnetizing (M-H) curves of this system is indicative of poor magnetic coupling between grains, which is also very consistent with the $-H_K$ shape observed in only weakly-interacting particulate systems.

The second peak observed in decreasing the field after positive saturation corresponds to the "crossover field", H_{cr}. In the introduction section, it was briefly stated that the cooling field required to change the shape of the temperature dependent magnetization curve from the drop in magnetization (figure 1a) to the increase in magnetization (figure 1b) roughly corresponds to 75 mT. We can now more precisely define H_{cr} as that field which separates the lower magnetization state from the higher magnetization state for any given temperature occurring below T_A and manifest as this peak in the TS profile. Since transverse susceptibility is a measure of the field-derivative of the magnetization, it makes sense that subtle changes in the M(T) curve should show up as well-defined peaks in this measurement, again indicating that TS is ideal for investigating unusual features in magnetic anisotropy that are not often picked up clearly in conventional magnetometry.

The third peak observed is the prominent switching peak, H_S. It is important to note that in the transverse susceptibility set-up, the signal is dominated by those crystallites whose easy axes of magnetization are perpendicular to the bias DC field. Therefore, the switching peak is not correlated simply with the maximum of the derivative of the M-H curve (as is the case for the parallel susceptibility measurement), which is a collective response contributed to by all crystallites. The parallel susceptibility measurement, (in which $H_{AC} \parallel H_{DC}$), does give the switching field as averaged over the entire sample. The peaks observed under the two different geometries therefore will not generally occur at the same field in polycrystalline samples.

Now that the peaks present have been identified, let us focus on the trends observed for the basic shape of the TS profile at the representative temperatures. The TS scans at 20K (figure

2a) and 95K (figure 2b) are fully consistent with other systems upon increasing the temperature. The anisotropy, switching, and crossover field peaks are sharp and well-defined at 20K. At 95K, the features become slightly more ambiguous and the curve becomes narrower in shape as the anisotropy features are shifted to lower fields. Figures 2a and 2b have the same x-axis scale so it is easy to see that the overall TS profile has become narrower with increasing temperature. This evolution from wide, sharp features to narrower, smaller features has been seen numerous times in TS studies of materials as their Curie temperature is approached [31-34]. However, this trend does not continue as the temperature increases across T_A, as it would if it were approaching a phase transition from, for example, an FM to a paramagnetic state. The structural transition is rather broad (as evidenced by the M(T) curves) and by 110K (figure 2c) already the TS curve has taken on a dramatically different shape than that seen at 95K. The peaks are once again very well-defined with features occurring at higher fields than even at lower temperatures. By 225K (figure 2d) the curve is once again narrower as the material approaches its Curie temperature (230K). It is interesting to note that by 225K the peak associated with the crossover field is gone, as the material has now entered the regime seen in the M(T) curves where the behavior is the same regardless of the cooling field. These four curves illustrate that for temperatures approaching T_A the TS evolves as expected for a material in increasing temperatures approaching a Curie temperature, however rather than passing through a Curie temperature, it passes through T_A, the result of which seems to be that the TS peak shape and width evolution seems to "start again" and this time evolve until the Curie temperature is reached. This is direct observation of evolution of the effective magnetocrystalline anisotropy in the system as it goes from one FM phase into another.

This point is more qualitatively illustrated by observing figure 3 in which we have superimposed the TS curves for each phase onto two separate plots. Figure 3a shows the temperature evolution of the TS curves for phase FM1 and figure 3b shows the temperature evolution of the TS curves for FM2. Unlike in figure 2, the magnitude of the TS signal appears in arbitrary units so that all the curves could be fit onto either graph in a manner that still clearly showed the features. What is remarkable is the degree to which the two phases differ in appearance. Whereas FM1 has a very well defined $+H_K$ peak for all temperatures up to the transition and displays the crossover field peak, the FM2 curve is largely dominated by the intense switching peak and the anisotropy peak appears much more broad. Separating the curves for FM1 and FM2 results in an appearance akin to the comparison of two different materials entirely, rather than the comparison of two phases of the same material. This clearly visible phase separation, which remains slightly ambiguous in the M(T) and doesn't exist at all in the family of M-H curves, is further indication that the TS measurement is ideal for studying anisotropy driven transitions.

The differences in anisotropy peak, switching peak, and crossover field peak between the two phases across the transition T_A are quantitatively examined in figure 4, where we present the field associated with each of these peaks as a function of temperature. Figure 4a shows the anisotropy field ($+H_K$) as a function of temperature where it is conclusively demonstrated that the FM2 phase of $Pr_{0.5}Sr_{0.5}CoO_3$ has a higher magnetocrystalline anisotropy than the lower temperature, FM1 phase. For lower temperatures ($T < T_A$,) the anisotropy field decreases with increasing temperature, which is typical of most magnetic systems as the thermal energy begins to compete with the anisotropy energy of the system. The structural transition at 120K here

appears as a dramatic increase in anisotropy field to values even higher than those seen at the lowest temperatures – $\mu_0 H_K \sim 184$ mT at 120K versus ~125 mT at 10K. The sharp change in H_K at T_A is a direct consequence of the coupled structural/magnetocrystalline anisotropy transition [27]. After reaching this maximum, H_K then slowly decreases again until T_C where it goes to zero.

The switching field (H_S) is tracked as a function of temperature in figure 4b. Its shape closely follows that reported in reference [27] (not shown) for both the coercivity and fraction of irreversible magnetization as measured by the first order reversal curve method [37]. This is not surprising as all three properties are direct consequences of irreversible hysteretic processes. At low temperatures it decreases rapidly until the approach to T_A where it experiences an uptick and a cusp at 120K and then decreases again until T_C.

Figure 4c shows the evolution of the peak position associated with the crossover field (H_{cr}) as a function of temperature. It has already been discussed that the presence of this peak lends insight to the crossover behavior between the two types of anomalous M(T) curves. While empirical data suggested this field to be around 75 mT, the temperature dependence of this peak reveals that this crossover field is different for different regions of the M(T) plots. Around the structural transition, the crossover field is indeed measured by TS to be 75 mT. However, at lower temperatures, the change in shape of the magnetization curves appears to occur at much lower fields, around 20 mT, which then increases rapidly with temperature up to T_A. Notice that unlike the other two peaks tracked across the transition, this crossover field does go to zero

shortly after the transition (rather than at T_C), which corresponds to where the M(T) curves display qualitatively identical behavior no matter the cooling field.

In figure 4d we have plotted the magnitude of the susceptibility signal for the switching peak as a function of temperature. The solid squares are for the transverse susceptibility scans where the phase transition at 120K can be clearly seen as a local minimum between the two phases. The open circles are data points taken of the switching peak using the parallel susceptibility method, where $H_{AC} \parallel H_{DC}$. This measurement is performed by simply rotating the coil that goes inside the magnet by 90°, so neither the circuit configuration nor the sample position within the coil has changed. As previously mentioned, the signal from the transverse susceptibility is dominated by those crystallites in the sample whose hard axes are aligned with the DC magnetic field. The parallel susceptibility measurement, basically the derivative of the M-H curve, has a signal essentially averaged over all orientations. It can be seen in figure 4d that for FM1 (low temperature phase) the magnitude of the signal obtained in the parallel configuration is larger than that obtained in the transverse configuration. This would imply that while there is significant signal from crystallites with the easy axis 90° from H_{DC}, the overall magnetic susceptibility is dominated by crystallites with their easy axes at angles other than 90° to H_{DC}. However, after the transition, while the signal from both orientations increases to that above the previous maximum, now the situation is reversed. The signal is much stronger coming from the crystallites with their hard axes along H_{DC} than the average switching peak orientation. Since the crystallites themselves are not changing orientation across the transition, their magnetization axes must be. This "crossover" behavior (not to be confused with H_{cr}) adds support to the notion that the anisotropy vector changes direction as well as magnitude, due to

the transition in a- and b-axis lattice parameters [27]. This is fully consistent with the previous observations using Lorentz microscopy [24] and traditional magnetometry [25] on single crystals of $Pr_{0.5}Sr_{0.5}CoO_3$ that indicate that a change in *direction* of the anisotropy vector occurs with the easy axis of magnetization rotating from [110] at higher temperatures to [100] at low temperature. While TS has been used in the past to observe similar reorientation of magnetization axis in Cr_2O_3/CrO_2 bilayer thin films [31], this represents the first time TS has been used to observe this phenomenon in a polycrystalline sample.

IV. CONCLUSIONS

We have used the transverse susceptibility measurement technique to examine the anisotropic magnetic properties of $Pr_{0.5}Sr_{0.5}CoO_3$, specifically the structure-driven magnetocrystalline anisotropy transition at 120K. We were able to show using this technique that the FM-FM phase transition is clearly manifest in the evolution of the anisotropy and switching peaks with temperature. The well-documented unusual M(T) behavior, dependent on cooling field, is present in the TS as well in form of a sharp peak at the crossover field which disappears above T_A. Lastly, we showed that the rotation of the easy axis can also be deduced by comparing the signal intensity from two different measurement orientations where a crossover behavior is observed. Collectively these findings show that transverse susceptibility is a very useful method for lending insight into the unusual magnetic behavior of doped perovskites.

ACKNOWLEDGEMENTS

Work at USF is supported by the Department of Energy through Grant No. DE-FG02-07ER46438

REFERENCES

[1] Y. Tomioka, A. Asamitsu, Y. Moritomo, H. Kuahara, and Y. Tokura, Phys. Rev. Lett. **74**, 5108 (1995).

[2] Y. Tokura and N. Nagaosa, Science 288, 462 (2000).

[3] E. Dagotto, Science 309, 257 (2005).

[4] A. J. Millis, P. B. Littlewood, and B. I. Shraiman, Phys. Rev. Lett. **74**, 5144 (1995).

[5] E. K. Abdel-Khalek, A. F. Salem, E. A. Mohamed, and A. A. Bahgat, J. Magn. Magn. Mater. **322**, 909 (2010).

[6] H. Kawano, R. Kajimoto, H. Yoshizawa, Y. Tomioka, H. Kuwahara, and Y. Tokura, Phys. Rev. Lett. **78**, 4253 (1996).

[7] Z. Q. Li, X. H. Zhang, H. Liu, X. D. Liu, W. B. Mi, H. L. Bai, X. N. Jing, and E. Y. Jiang, Sol. St. Comm. **130**, 563 (2004).

[8] S. W. Cheong and M. Mostovoy, Nat. Mater. **6**, 13 (2007).

[9] D. I. Khomskii, J. Magn. Magn. Mater. **306**, 1 (2006).

[10] E. Dagotto, Nanoscale Phase Separation and Colossal Magnetoresistance (Springer, New York, 2002).

[11] S. Cao, B. Kang, J. Zhang, and S. Yuan, Appl. Phys. Lett. **88**, 172503 (2006).

[12] P. Schiffer, A. P. Ramirez, W. Bao, and S.-W. Cheong, Phys. Rev. Lett. **75**, 3336 (1995).

[13] Y. Ji, C. L. Chien, Y. Tomioka, and Y. Tokura, Phys. Rev. B **66**, 012410 (2002).

[14] B. Nadgorny, I. I. Mazin, M. Osofsky, R. J. Soulen, Jr., P. Broussard, R. M. Stroud, D. J. Singh, V. G. Harris, A. Arsenov, and Ya. Mukavskii, Phys. Rev. B **63**, 184433 (2001).

[15] M.-H. Phan and S.-C. Yu, J. Magn. Magn. Mater. **308**, 325 (2007).

[16] N. S. Bingham, M.-H. Phan, H. Srikanth, M. A. Torija, and C. Leighton, J. Appl. Phys. **106**, 023909 (2009).

[17] C. N. R. Rao and B. Raveau (Editors), Colossal Magnetoresistance, Charge Ordering and Related Properties of Manganese Oxides World Scientific, Singapore (1998); *Colossal Magnetoresistance Oxides,* edited by Y. Tokura, Monographs in Condensed Matter Science (Gordon and Breach, New York, 1999).

[18] V. B Shenoy and C.N.R Rao, Phil. Trans. R Soc. A 366, 63 (2008) J. M. D. Coey, M. Viret, and S. von Molnár, Adv. Phys. **48**, 167 (1999).

[19] A. Podlesnyak, S. Streule, J. Mesot, M. Medarde, E. Pomjakushina, K. Conder, A. Tanaka, M. W. Haverkert, and D. I. Khomskii, Phys. Rev. Lett. **97**, 247208 (2006).

[20] D. P. Kozlenko, N. O. Golosova, Z. Jirák, L. S. Dubrovinsky, B. N. Savenko, M. G. Tucker, Y. Le Godec, and V. P. Glazkov, Phys. Rev. B **75**, 064422 (2007).

[21] R. F. Kile, J. C. Zheng, Y. Zhu, M. Varela, J. Wu, and C. Leighton, Phys. Rev. Lett. **99**, 047203 (2007).

[22] K. Yoshii, A. Nakamura, H. Abe, M. Mizumaki, and T. Muro, J. Magn. Magn. Mater. **239**, 85 (2002).

[23] R. Mahendiran and P. Schiffer, Phys. Rev. B **68**, 024427 (2003).

[24] M. Uchida, R. Mahendiran, Y. Tomioka, Y. Matsui, and K. Ishizuka, Appl. Phys. Lett. **86**, 131913 (2005).

[25] S. Hirahara, Y. Nakai, K. Miyoshi, K. Fujiwara, and J. Takeuchi, J. Magn. Magn. Mater. **310**, 1866 (2007).

[26] M. Patra, S. Majumdar, and S. Giri, J. Appl. Phys. **107**, 033912 (2010).

[27] C. Leighton, D. D. Stauffer, Q. Huang, Y. Ren, S. El-Khatib, M. A. Torija, J. Wu, J. W. Lynn, L. Wang, N. A. Frey, H. Srikanth, J. E. Davies, K. Liu, and J. F. Mitchell, Phys. Rev. B **79**, 214420 (2009).

[28] H. Srikanth, J. Wiggins, and H. Rees, Rev. Sci. Instrum. **70**, 3097 (1999).

[29] We identify certain commercial equipment, instruments, or materials in this article to specify adequately the experimental procedure. In no case does such identification imply recommendation or endorsement by the National Institute of Standards and Technology, nor does it imply that the materials or equipment identified are necessarily the best available for the purpose.

[30] A. Aharoni, E. H. Frei, S. Shtrikman, and D. Treves, Bull. Res. Counc. Isr., Sect. F **6A**, 215 (1957).

[31] N. A. Frey, S. Srinath, H. Srikanth, M. Varela, S. Pennycook, G. X. Miao, and A. Gupta, Phys. Rev. B **74**, 024420 (2006).

[32] G. T. Woods, P. Poddar, H. Srikanth, and Ya. M. Mukovskii, J. Appl. Phys. **97**, 10C104 (2005).

[33] R. Swaminatham, M. E. McHenry, P. Poddar, and H. Srikanth, J. Appl. Phys. **97**, 10G104 (2005).

[34] P. Poddar, M. B. Morales, N. A. Frey, S. A. Morrison, E. E. Carpenter, and H. Srikanth, J. Appl. Phys. **104**, 063901 (2008).

[35] P. V. Patanjali, P. Theule, Z. Zhai, N. Hakim, S. Sridhar, R. Suryanarayanan, M. Apostu, G. Dhalenne, A. Revcolevschi, Phys. Rev. B 60, 9268 (1999).

[36] V. B. Naik and R. Mahendiran, Appl. Phys. Lett. **94**, 142505 (2009).

[37] C. R. Pike, Phys. Rev. B **68**, 104424 (2003).

FIGURE CAPTIONS

FIG. 1. Magnetization versus temperature measured upon cooling for several applied fields. (a) H=10 Oe where there is a decrease in magnetization with decrease in temperature below 120K. (b) H = 1kOe where there is an increase in magnetization with decrease in temperature. The 120K anomaly is visible. (c) H = 50 kOe where no anomaly can be detected.

FIG. 2. Bipolar transverse susceptibility scans of $Pr_{0.5}Sr_{0.5}CoO_3$ as a function of applied field for 20K (a), 95K (b), 110K (c), and 225K. On 2(a) the arrows indicate the sequence of measurement and the anisotropy (H_K), crossover (H_{cr}), and switching (H_S) peaks are labeled.

FIG. 3. Unipolar transverse susceptibility scans for several different temperature plotted on two plots depicting the two different ferromagnetic phases ((a) is FM1 and (b) is FM2). The signal intensity appears in arbitrary units as soon of the curves have been shifted upward or downward for clarity.

FIG. 4. Temperature dependence of the peaks positions in the transverse susceptibility measurement. (a) Anisotropy field ($+H_K$) position versus temperature. (b) Switching field (H_S) position versus temperature. (c) Crossover field (H_{cr}) position versus temperature. All three graphs show local maxima at the 120K transition.

FIG. 5. Switching field peak intensity $(\Delta\chi/\chi)_{max}$ as a function of temperature taken using two different geometries. The open circles are from parallel susceptibility scans and the solid circles are from transverse susceptibility scans. That the relative signal intensities undergo a crossover around the transition temperature is an indication that the anisotropy axis rotates during the structural transition.

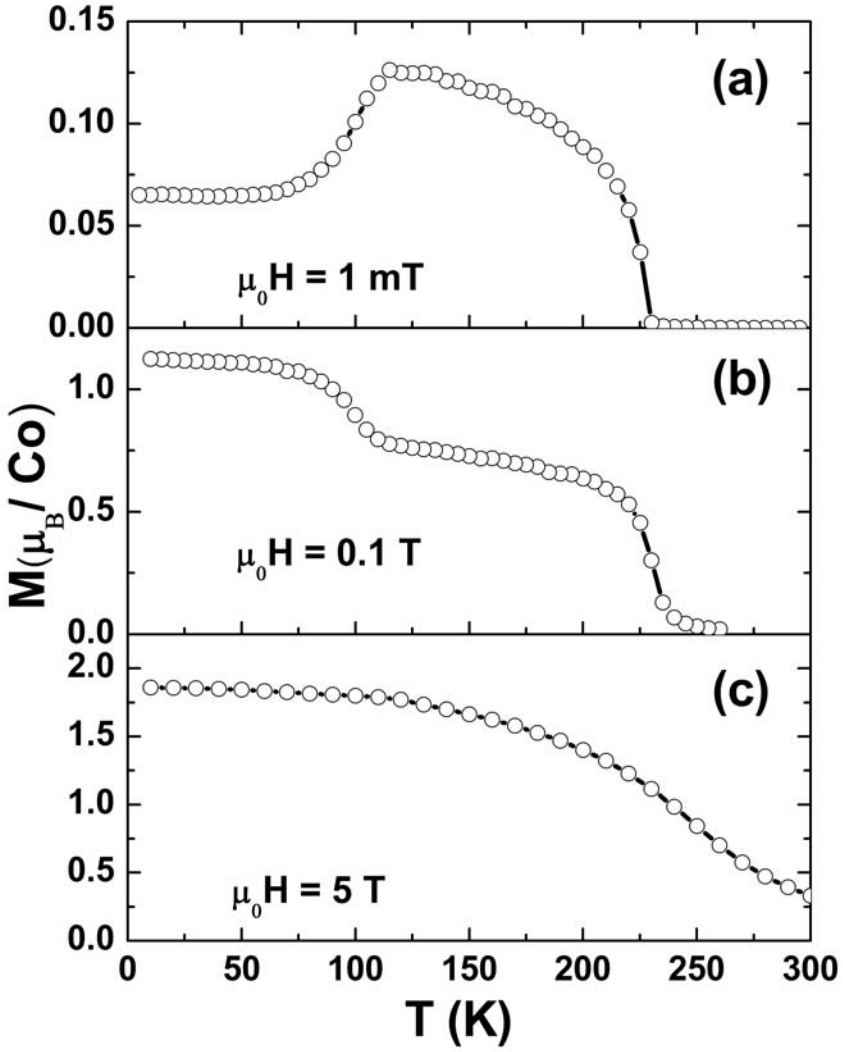
0.15
0.10
0.05
0.00
(a)
μ_0H = 1 mT
1.0
0.5
0.0
(b)
μ_0H = 0.1 T
2.0
1.5
1.0
0.5
0.0
(c)
μ_0H = 5 T
M(μ_B / Co)
0
50
100
150
200
250
300
T (K)

Figure 1.

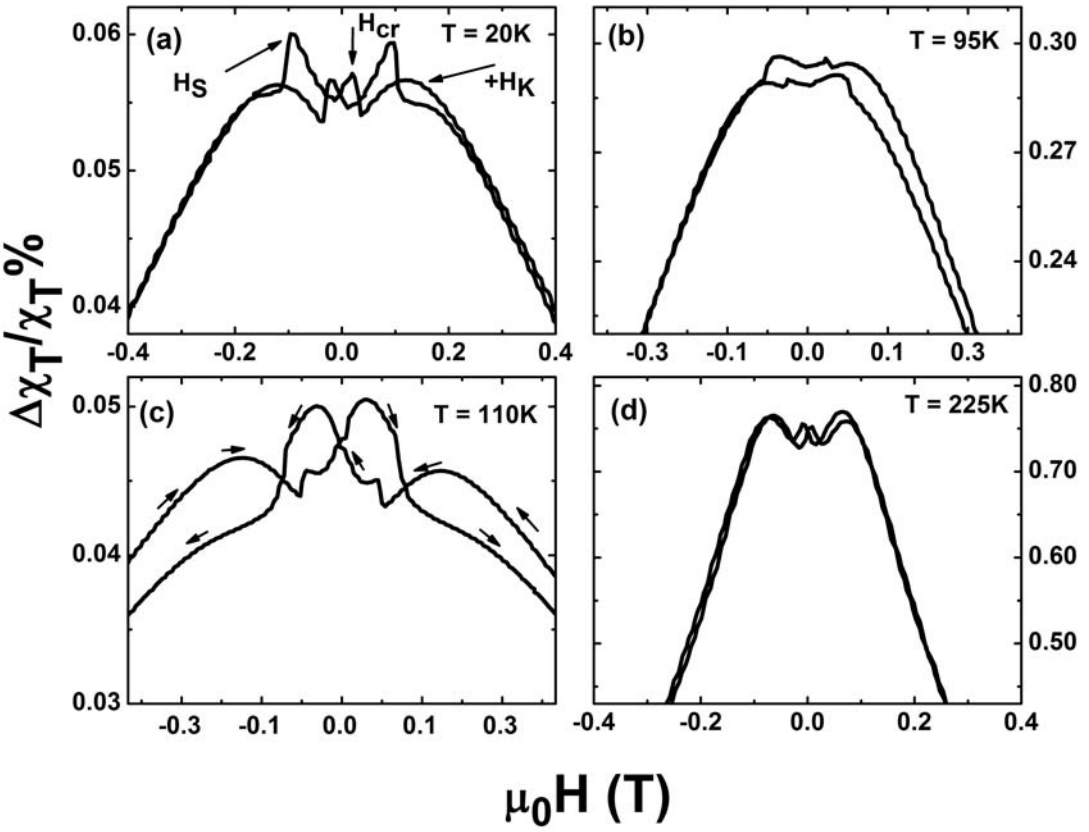

Figure 2.

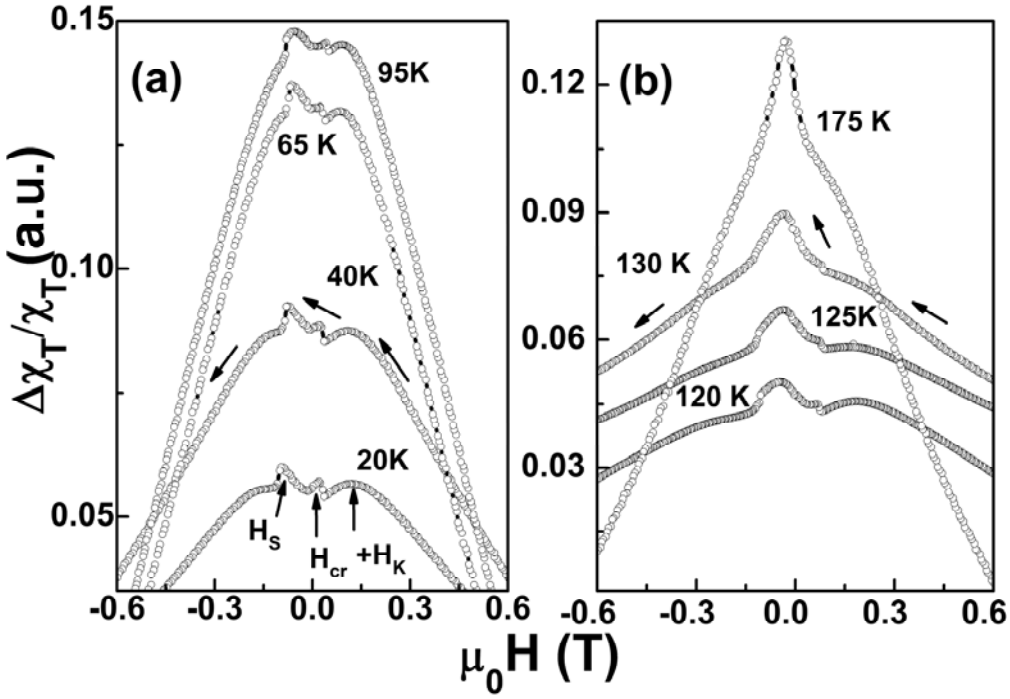
(a)
95K
65 K
40K
20K
H_S
H_{cr}
$+H_K$
(b)
175 K
130 K
125K
120 K
$\Delta\chi_T/\chi_T$(a.u.)
$\mu_0 H$ (T)

Figure 3.

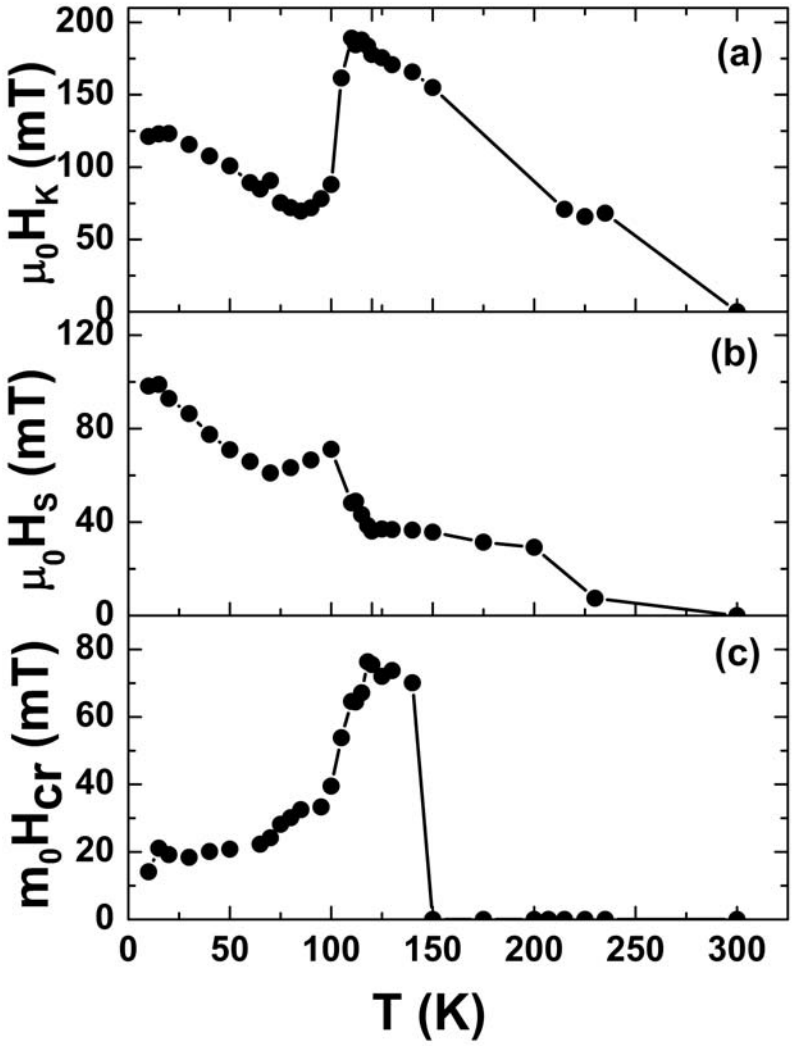
(a)
(b)
(c)
$\mu_0 H_K$ (mT)
$\mu_0 H_S$ (mT)
$m_0 H_{cr}$ (mT)
T (K)
0
50
100
150
200
250
300
0
20
40
60
80
120

Figure 4.

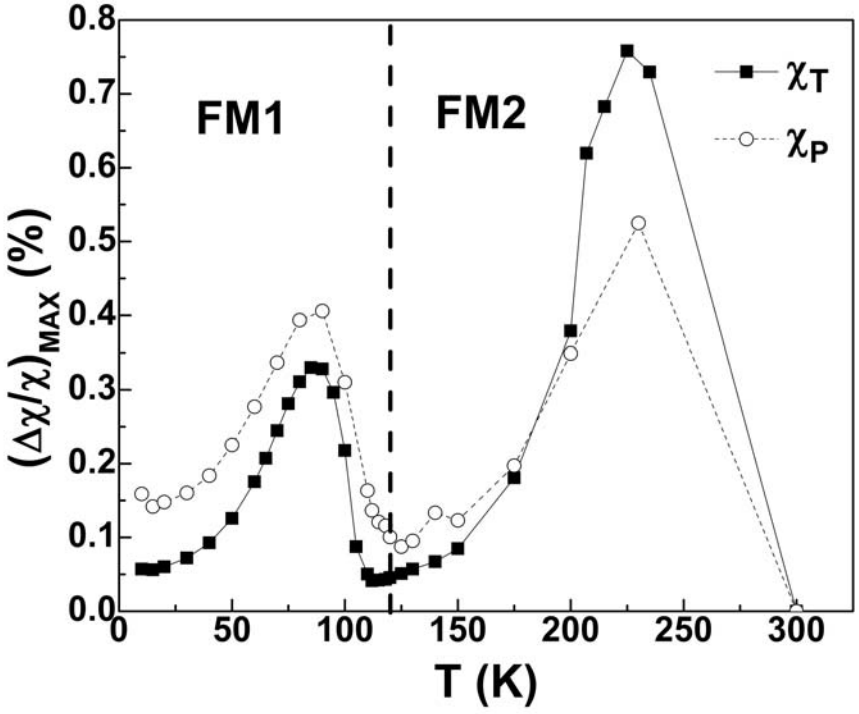
FM1
FM2
χ_T
χ_P
$(\Delta\chi/\chi)_{MAX}$ (%)
T (K)
0.0
0.1
0.2
0.3
0.4
0.5
0.6
0.7
0.8
0
50
100
150
200
250
300

Figure 5.